AD NUMBER

AD831376

NEW LIMITATION CHANGE

TO

Approved for public release, distribution unlimited

FROM

Distribution authorized to U.S. Gov't. agencies and their contractors; Administrative/Operational Use; Feb 1968. Other requests shall be referred to the Commanding Officer, Fort Detrick, Attn: Technical Release Branch Information Division, Fort Detrick, Frederick, MD.

AUTHORITY

BDRL D/A ltr, 29 Sep 1971

TECHNICAL MANUSCRIPT 430

PNEUMONIC PLAGUE IN MONKEYS: AN ELECTRON MICROSCOPE STUDY

Milton J. Finegold

FEBRUARY 1968

DEPARTMENT OF THE ARMY
Fort Detrick
Frederick, Maryland

33

DEPARTMENT OF THE ARMY
Fort Detrick
Frederick, Maryland 21701

TECHNICAL MANUSCRIPT 430

PNEUMONIC PLAGUE IN MONKEYS: AN ELECTRON MICROSCOPE STUDY

Milton J. Finegold

Pathology Division
MEDICAL SCIENCES LABORATORY

Project 1C522301A059 February 1968

In conducting the research described in this report, the investigators adhered to the "Guide for Laboratory Animal Facilities and Care," as promulgated by the Committee on the Guide for Laboratory Animal Facilities and Care of the Institute of Laboratory Animal Resources, National Academy of Sciences-National Research Council.

ACKNOWLEDGMENTS

The author is grateful to Dr. Richard Berendt, John Petery, and Captain Henry R. Adams, VC, for exposure of the animals to the aerosols and other invaluable assistance. Dr. John D. White and Dr. Michael J. Surgalla provided stimulation and consultation at every stage. Mrs. Frances Shirey rendered excellent technical assistance.

ABSTRACT

The infection of monkey lungs by Pasteurella pestis was studied with the electron microscope. The disease was first apparent clinically at 60 to 70 hours and pathologically at 72 hours. At this time, the initial response seen with the light microscope was alveolar edema with massive proliferation of organisms. With the electron microscope, interstitial edema around veins and bronchi was the earliest observed response to the presence of numerous intra-alveolar bacilli. Early in the disease, before the onset of a leukocytic exudate, interstitial fluid also accumulated in the form of subepithelial blebs. No evidence of significant vascular damage was found to account for the marked increase in permeability, even with the aid of intravenous injections of colloidal carbon prior to sacrifice. Leukocytic and mast cell factors in the pathogenesis of the edema appear unlikely. Once the cellular component of the reaction developed, P. pestis resisted both phagocytosis by polymorphonuclear neutrophils and intracellular digestion by mononuclear phagocytes. Invasion of the tissues by the organism was observed only in the advanced stages of the pneumonia, when all components of the alveolar septa were undergoing necrosis.

CONTENTS

APPENDIX

TABLE

I. INTRODUCTION

Pneumonic plague is characterized by extensive intra-alveolar edema containing myriads of Pasteurella pestis prior to any significant leukocytic exudate or damage to lung tissue,[1] when studied by light microscopy. Infected edema fluid is also found at the margins of consolidated areas and is the initial change in secondary lesions.[1] Other bacterial pneumonias, such as pneumococcal, seem to have a similar pathogenesis, both in the rare human cases with abbreviated disease due to intervening accident[2] and in experimental animals,[3] but they differ from plague in the more rapid addition of leukocytes, fibrin, and red blood cells to the exudate.

The electron microscope has been successfully employed in the study of a variety of inflammatory reactions and their components, such as leukocyte migration,[4] phagocytosis,[5,6] and vascular permeability,[7] but there have been few reports of the ultrastructural manifestations of bacterial pneumonia.[8-12] In view of the value of electron microscopy in detecting tissue damage in experimental pulmonary edema prior to the appearance of lesions visible with the light microscope,[8,9] it seemed appropriate to examine the lungs of animals exposed to aerosols of P. pestis in order to describe the ultrastructural changes in necrotizing pneumonia and, hopefully, to determine the pathogenesis of the extensive, early edema.

II. MATERIALS AND METHODS

A. ANIMALS

Rhesus monkeys (Macaca mulatta) imported from India were housed locally for at least 90 days before use. Young adults of both sexes weighing between 2.6 and 3.25 kg were housed in pairs and were fed Purina monkey chow* and water ad libitum. Tuberculin testing was performed monthly, and only negative reactors were used.

B. ORGANISM AND EXPOSURES

The KIM-10 strain of P. pestis was used. The isolation, maintenance, and cultural characteristics have been described,[13] as have the methods of aerosol generation, animal exposure, and dosimetry. The calculated inhaled dose in these experiments averaged 1360 bacilli per monkey.

* Ralston Purina Co., St. Louis, Mo.

C. SAMPLING

Pairs of monkeys were chosen at random at 6, 12, 24, 48, 72, and 96 hours post-exposure to P. pestis aerosols. Each monkey was injected intramuscularly with Sernylan,®* 2.0 mg per kg of body weight, which produced stupor within 10 to 15 minutes. One of each pair then was given an intravenous injection of colloidal carbon,** 0.1 g per 100 g of body weight. Three to 5 minutes later, the monkeys were sacrificed with intravenous pentobarbital.

D. TISSUE PREPARATION

Immediately after the pentobarbital injection, the chest was opened and the lungs were excised. They were dissected free of mediastinal tissues and weighed. They were fixed by endotracheal perfusion of cold 2% glutaraldehyde buffered to pH 7.2 by 0.1 M phosphate to give a total osmolality of 444 milliosmols. The perfused lungs were immersed in the same fluid at 0 to 4 C for 1 hour, then examined grossly and sectioned. Five to ten 1-mm cubes of tissue from representative areas of each lung were taken for electron microscopic examination, and sections of all lobes measuring 2 by 1 by 0.4 cm were excised for paraffin embedding and light microscopy. The latter sections were 5- to 7-μ thick and were stained with hematoxylin-eosin and Giemsa's stain. Processing for electron microscopy consisted of washing in phosphate buffer adjusted to 444 milliosmols with 0.25 M sucrose, mincing in buffer, fixing in 1% osmium tetroxide for 1 hour, dehydrating in graded alcohols, embedding in Epon 812, sectioning at 400 to 800 Å with a Porter-Blum MT 1 microtome, treating sections on unsupported copper grids with a saturated solution of uranyl acetate, and viewing in a RCA EMU 3-G microscope.

* Parke, Davis & Co., Detroit, Mich.

** Pelikan C 11/1431a, Gunther-Wagner Co., Hanover, Germany.

III. RESULTS

A. CLINICAL COURSE AND ROUTINE PATHOLOGY

The clinical course and routine pathological findings are summarized in Table 1. Until approximately 60 hours post-exposure, there were no clinical signs of infection, so that the eight monkeys sacrificed prior to 72 hours appeared healthy, with no remarkable findings in the lungs on gross or microscopic examination.

The remaining four monkeys developed temperatures of 104 to 105.3 F between 60 and 72 hours post-exposure and had slight tachypnea (respiratory rate of 60 to 70 per minute). They were otherwise clinically well, with no lethargy or loss of appetite. This is similar to previous studies on pneumonic plague in monkeys.[14] At necropsy, the lungs of one of the 96-hour monkeys (No. 11) were considerably heavier than normal, and those of the other 96-hour monkey (No. 12) appeared slightly heavier, when compared with body weight (Table 1).

All four monkeys sacrificed at 72 and 96 hours had pneumonia, the most extensive being confluent gray hepatization of the right lower lobe of monkey No. 10. There was central liquefactive necrosis of this area, and the overlying pleura was dull and opaque with hemorrhagic foci. An area of increased consistency and excess fluid was present in the left upper lobe of this monkey, and similar foci, consistent with early lobular pneumonia, were found in the other three monkeys.

Microscopically, each of the four monkeys examined at 72 and 96 hours had pneumonia, with a range of lesions in each animal that conformed to the many earlier descriptions of the disease in both man and animals.[1,15] The mildest infection was found in monkey No. 12 and consisted of extensive alveolar edema containing numerous bacilli and a variable leukocytic infiltrate of the septa and alveoli (Fig. 1 to 3).* In some areas, there were very few polymorphonuclear neutrophils within septal capillaries, but individual alveoli elsewhere were filled with the same cells. No changes in the alveolar walls could be detected initially (Fig. 3), but, after examining the electron micrographs, it was possible to recognize sub-epithelial blebs in the areas of edema with the light microscope. They consisted of rounded elevations of the alveolar wall, 7- to 12-μ in diameter, that contained eosinophilic fluid. Their origin could be ascertained only with the electron microscope (see below). Perivascular and peribronchial lymphatics in the vicinity of the early lesions were distended with fluid. Bronchi and terminal bronchioles were not remarkable. The same histologic appearance characterized the secondary lesions in monkeys No. 10 and 11.

* See Appendix.

TABLE 1. CLINICAL AND PATHOLOGICAL RESPONSES OF MONKEYS TO AEROSOLS OF *P. PESTIS*

Animal No.	Sacrifice, hours post-exposure	Clinical Symptoms	Lung Weight (g) / Body Weight (kg)	Pathology	
				Gross[a]	Microscopic
1	6	-	7.6	-	-
2	6	-	-	-	-
3	12	-	8.6	-	-
4	12	-	8.7	-	-
5	24	-	8.7	-	-
6	24	-	8.6	-	-
7	48	-	6.6	-	-
8	48	-	6.5	-	-
9	72	Fever tachypnea	8.8	LUL perihilar edema	Lobular pneumonia
10	72	Fever tachypnea	9.1	LUL edema; RLL consolidation	Early pneumonia; necrotizing pneumonia
11	96	Fever tachypnea	14.5	LUL, LLL edema; RLL consolidation	Early pneumonia; necrotizing pneumonia
12	96	Fever tachypnea	9.7	LLL perihilar edema	Early lobular pneumonia

a. LUL = left upper lobe; LLL = left lower lobe; RLL = right lower lobe.

More advanced lobular pneumonia consisted of: alveolar consolidation by polymorphonuclear neutrophils and a few mononuclear cells; extensive infiltration of septa, interlobular, peribronchial, and perivascular connective tissue by the same cells; massive growth of bacilli in the alveoli and lymphatics; and foci of inflammation and necrosis of bronchiolar epithelium. Hemorrhages and focal necrosis of the alveolar septa were numerous in the centers of the confluent areas of pneumonia (Fig. 4).

The carbon injections did not reveal the site of increased vascular permeability. Prior to 72 hours, the only evidence of the presence of carbon consisted of diffuse black stippling of the blood in large vessels. In animals No. 10 and 11, discrete aggregates of carbon occluded arterioles and capillaries, both in the areas of pneumonia and elsewhere. No carbon was detected in the alveolar edema fluid or in lymphatics.

B. ELECTRON MICROSCOPY

With the aid of routine histologic sections and 1-μ-thick toluidine-blue-stained sections of each capsule of plastic-embedded tissue, it was possible to select, for study with the electron microscope, areas of the lung that represented a progression from minimal to maximal alterations of the normal morphology. The progression is assumed to reflect the temporal sequence of inflammation, and the observations will be presented according to that interpretation.

No ultrastructural alterations in lung morphology were observed prior to 72 hours. Numerous sections from the 6-hour and 48-hour monkeys were examined with special diligence in an effort to locate P. pestis in the periods soon after exposure to the aerosol and just preceding the onset of frank pneumonitis. Although the sections included portions of distal bronchi, bronchioles, alveoli, venules, veins, and lymphatics, neither organisms nor changes in the tissues were observed.

1. Edema

Sections from the areas of alveolar edema found by light microscopy showed numerous plague bacilli in the alveoli but none in the tissue. There were many areas with no morphologic changes despite the presence of the organisms. Fluid in the alveoli was not sufficiently dense to be recognized. Interstitial edema could be detected by its effects in separating normal structure and was the earliest tissue alteration to be recognized. Perivascular and peribronchial connective tissues were widened by finely granular material that ranged in opacity from that of background (Fig. 15, 16, 27 and 28) to that of plasma (Fig. 24 and 2?). Interstitial fluid also accumulated beneath the thin segments of the aveolar epithelium (Type I cell), resulting in large blebs or blisters (Fig. 5) that were also visible with the light microscope. In some

sections, it was impossible to determine whether the fluid was extracellular or within a large intracellular vacuole (Fig. 5 and 7). However, other sections clearly revealed continuity of the fluid with the interstitial space (Fig. 6). Although affected alveolar epithelial cells were strikingly attenuated by the blisters, they were not remarkable otherwise. Some cells showed a few small cytoplasmic vacuoles in the areas with the blebs (Fig. 7). Some blebs in the areas having a cellular infiltrate also contained leukocytes (Fig. 6) or erythrocytes (Fig. 7); however, carbon was rarely found in the blebs, even when present in nearby vessels. As the pneumonia progressed, interstitial edema became more extensive and spread from the peritruncal areas to the thin portions of the septa. At this time, blebs were no longer seen.

2. Endothelial Lesions

The capillary endothelium showed minimal, focal, cytoplasmic alterations in the areas of edema. Swelling of the cells with rarefaction of the cytoplasmic matrix was seen rarely in the early stages but became common in the more inflamed areas. This change often was restricted to part of a single cell, leaving organelles and pinocytotic vesicles intact (Fig. 9), and was therefore considered to be a degenerative phenomenon. Other early endothelial changes consisted of the formation of multivesicular bodies (Fig. 9 and 10), lipid vacuoles (Fig. 11), and cytoplasmic inclusions of indeterminate nature (Fig. 10 and 11). The appearance of membrane-like structures, or myelin figures, within the cytoplasm may indicate degeneration of some of the internal membranes of the cell. No increase in the number or size of the pinocytotic vesicles was noted at any stage.

More advanced endothelial damage was found in the areas of necrosis, where all elements of the tissue were involved. These changes consisted of swelling of the cell, opacification of the cytoplasmic matrix, vacuolization of mitochondria, and disruption of the cell membrane (Fig. 12). No intravascular thrombi were observed at any time during this study, and even when small vessels were plugged with carbon, the occasional platelet in the area appeared intact and retained its granules. No fibrin was found.

3. Cellular Exudate

Extravasation of erythrocytes was noted in some areas with both the light (Fig. 1) and electron (Fig. 7 and 8) microscopes. Very infrequently, an erythrocyte was observed leaving a capillary for the interstitial space (Fig. 12). A gap in the endothelial lining was associated with alterations in the cytoplasm of the cells at the site, which appeared more dense and homogenous than normal with no vesicles. Otherwise, the tissue in these areas appeared unaltered. No erythrocytes were found emerging from veins or venules.

Leukocyte migration could be traced from capillaries and more often from venules into the interstitium and thence into the alveoli (Fig. 14 to 19). Polymorphonuclear neutrophils and monocytes appeared simultaneously within vessels (Fig. 8), in the interstitium (Fig. 8, 16 and 17), and in the alveoli (Fig. 19), although neutrophils outnumbered monocytes throughout the period of this study. Eosinophils (Fig. 19) were found in the more intensely inflamed and necrotic areas. Lymphocytes and plasma cells were not part of the reaction. The passage of leukocytes through the vessel walls was accompanied by either no change or minor alterations of the endothelium (Fig. 14 and 15), and the defects appeared to be between cells. Gaps permitting the migration of leukocytes out of vessels also allowed the egress of carbon (Fig. 15), which otherwise was confined to the blood plasma or to cytoplasmic vacuoles of monocytes. The cytoplasm of alveolar epithelial cells at the sites of leukocytic migration was homogenously granular and devoid of pinocytotic vesicles (Fig. 18), just as was the endothelium.

4. Interactions of Leukocytes and Organism

Neutrophils were plentiful in vessels, interstitium, and alveoli, and, in the latter site, were in proximity to many plague bacilli (Fig. 22), yet phagocytosis by neutrophils was very rarely observed. Once in the interstitium or alveoli, some neutrophils had cytoplasmic vacuoles (Fig. 8, 16 and 17), but others appeared degranulated without the formation of vacuoles (Fig. 18). Monocytes did phagocytize P. pestis (Fig. 20 and 21), as well as leukocytes (Fig. 20), erythrocytes, phospholipid profiles, and other debris. Lysosomes and phagocytic vacuoles were inconspicuous until the cells reached the interstitium or alveoli. The outcome of phagocytosis of the bacilli was generally unfavorable to the monocyte (Fig. 22 and 23), although a bacillus occasionally appeared to be undergoing digestion (Fig. 21).

5 Epithelial Lesions

The alveolar epithelium displayed little early response to the presence of numerous P. pestis in the lumen. Only in the areas of intense inflammation did the lining cells show morphological abnormalities. These consisted of: focal swelling of the endoplasmic reticulum of both the granular (Type II) pneumoncyte (Fig. 24) and the squamous (Type I) epithelial cell (Fig. 25); mitochondrial swelling with loss of cristae (Fig. 25); rarefaction of the cytoplasmic matrix (Fig. 25); and, finally, sloughing of the cell, leaving exposed basement membrane (Fig. 26).

6. Mast Cells

Normal-appearing mast cells were present in the adventitia of veins and venules early in the pneumonitis, when edema was the predominant feature (Fig. 27). Later, when leukocytic exudation was active, some mast

cells had empty granules (Fig. 28). They joined in the general process of necrosis, with fragmentation of cytoplasm and disruption of the cell membrane in the advanced lesions.

IV. DISCUSSION

For approximately 60 hours post-exposure to aerosols of P. pestis, the monkeys exhibited no clinical signs of infection. This was correlated with the absence of tissue alterations during the first 48 hours of the serial sacrifice experiment, as shown by both light and electron microscopy. By 72 hours post-exposure, the monkeys developed fever and mild tachypnea, and their lungs contained areas of lobular pneumonia. The failure to find organisms in the tissue prior to this time is disappointing but hardly surprising. One reason is that P. pestis, like other bacteria administered in an aerosol,[16,17] virtually disappears during the first few hours post-exposure. Smith et al.[18] estimated that only 5% of a calculated inhaled dose was recovered from the lungs of mice by culture 16 hours post-exposure. Meyer[19] reported approximately 10% recovery in guinea pigs 12 hours post-exposure. Applying their figures to the present experiment, approximately 100 plague bacilli would have been expected in the lungs at 12 to 16 hours post-exposure. When this estimate is considered in light of the problem of sampling for the electron microscope (in which the total volume of tissue included in the 250 to 500 thin sections examined from each pair of lungs approximated 0.00025 cubic mm), the chance of finding organisms prior to an advanced degree of proliferation is indeed infinitesimal. Thus, the question of the location of the bacilli during the pre-inflammatory stages of infection remains where it was left by Domaradskii.[20] Two hours following the exposure of guinea pigs to an aerosol, bacilli were seen in bronchi and alveoli of the medial portions of the lung near the hilus, but only a few bacilli could be seen by 5 hours, and they were within macrophages. At 24 hours, bacilli were present only in vacuoles of macrophages. They were not traced thereafter.

Our primary interest in studying the early stages of pneumonia was to determine the pathogenesis of the edema. Electron microscopy confirmed the earlier finding[1] that a serous exudate precedes the appearance of leukocytes in the tissues and further revealed that the first leukocytes to appear in the interstitial tissue and alveoli possessed intact granules. Thus, it is unlikely that leukocyte permeability factors of the sort described by Movat and co-workers[21] or other lysosomal substances[22] are responsible for the early increase in vascular permeability. Similarly, there is no support for the possibility that mast cells, with their content of vasoactive amines, heparin, and proteolytic enzymes,[3] have a significant influence on the early onset of edema because the many mast cells found

in the adventitia of veins and venules during the early stages had numerous intact granules. Later in the disease, some of the cells displayed empty granules, which is one method for release of their content,[23] but this can only be considered a secondary development.

There was no morphologic evidence for significant vascular damage as an initial response to infection. Although there were a few capillary endothelial cells with swollen rarefied cytoplasm and others with a variety of intracellular inclusions, similar changes were present in the areas without edema as well, and all were too uncommon early in the infection to account for the massive outpouring of fluid in some locations. Carbon particles having an average diameter of 250 Å could not be traced through or between endothelial cells of veins or capillaries until large gaps opened for the passage of leukocytes or erythrocytes. The failure to detect defects with carbon is similar to Florey's experience[24] with ferritin in the inflamed colon of the rat, but differs from Marchesi's observation[25] that colloidal carbon passed through intracellular junctions of venule endothelium in mildly traumatized rat mesentery. A tracer of considerably smaller size, such as the peroxidase of Karnovsky,[26] would seem more appropriate in future efforts to detect the sites of increased vascular permeability. No increase in the size or number of pinocytotic vesicles was found, as has generally been the case.[27]

The plague bacillus may be directly responsible for edema without invoking the participation of an endogenous mediator. The precedent for such a possibility was established many years ago for the pneumococcus by Sutliff and Friedemann,[28] who isolated a soluble product of the coccus that provoked edema in both the skin and lungs of dogs and helped to explain the propensity of pneumococcal pneumonia to spread rapidly throughout an entire lobe. In the case of P. pestis, Schär and Meyer[29] used the protein murine toxin from the bacillus to produce in mice by intranasal inoculation a pneumonitis that strongly resembled the early stages of plague pneumonia with interstitial edema followed by leukocytic exudation, necrosis, and hemorrhage. The murine toxin is relatively non-toxic for monkeys and most other species except mice and rats,[30] but other components of P. pestis might have similar effects. Interstitial pneumonitis (characterized by massive alveolar septal edema, foci of capillary hemorrhage, and a cellular reaction consisting of neutrophils, mononuclear phagocytes and eosinophils) was produced in rabbits 24 hours post-exposure to aerosols containing Escherichia coli endotoxin.[31] Recent studies suggest that endotoxin may have a significant role in experimental[13,32] and human[33] plague by causing intravascular coagulation with disseminated fibrin thrombi. There have been increasing efforts recently to isolate toxic lipopolysaccharides from P. pestis.[34] The delay between the onset of a logarithmic growth rate of the organism at 6 to 12 hours after infection[35] and the appearance of edema some 48 to 60 hours later may indicate that it is necessary for a certain quantity of toxin to accumulate in the tissues before edema is produced.

The resistance of _P. pestis_ to phagocytosis by polymorphonuclear neutrophils was observed with the electron microscope in this study. Previous studies demonstrated that _P. pestis_ acquires resistance to phagocytosis by neutrophils after a certain period of infection.[36] Furthermore, neutrophils fail to ingest phagocytosis-sensitive bacilli following exposure to virulent organisms.[36] Plasma from guinea pigs moribund with plague sepsis inhibits phagocytosis of sensitive bacilli by normal neutrophils in vitro.[37] In addition to these acquired factors that impair cellular responses to infection, the ingestion of bacilli by phagocytes does not insure digestion of the organism. Few examples of morphologic damage to bacilli within macrophages were seen, but many alveolar macrophages containing intact bacilli were found in various stages of degeneration. This substantiates previous conclusions[38] that the resistance of _P. pestis_ to intracellular digestion may have greater significance for the virulence of the organism than its resistance to phagocytosis.

The inflammatory and necrotic lesions described here for pneumonic plague are of interest because there have been no reports of bacterial pneumonias studied with the electron microscope. The changes represent a composite of the various inflammatory processes studied in many experimental situations.[4-7] Many of the pulmonary lesions have been described in viral pneumonitis,[39] toxic edema,[12] and in response to changes in the oxygen content of inspired air.[11] Previous studies of bacterial pneumonia with the electron microscope have dealt with the granulomatous response to tubercle bacilli[8,10] and with the early exudation of leukocytes in mice exposed to pneumococci.[9] The latter report presents photographs of leukocytes passing out of capillaries between endothelial cells, just as in plague, and it mentions, but does not depict, blebs in the alveolar epithelial membrane early in the infection. The possibility that similar electron micrographs are obtained from such a variety of studies because common artifacts result from similar processing techniques is unlikely because there are significant differences as well. For example, osmotic effects may account for alveolar epithelial cell swelling and vacuolization in pneumonic plague, as well as in fresh water drowning,[40] inhalation of carbon monoxide,[41] or poisoning of rats with alpha-naphthylthiourea,[42] but the subendothelial fluid accumulations found in those studies and in staphylococcal enterotoxicity[12] and oxygen toxicity[11] are not found in plague. Therefore, instead of attributing similar lesions to mistreatment of the tissues, it appears more likely that the lung can respond to a variety of noxious stimuli in but a few ways.

LITERATURE CITED

1. Strong, R.P.; Teague, O. 1912. Studies on pneumonic plague and plague immunization: IV. Portal of entry of infection and method of development of the lesions in pneumonic and primary septicemic plague; experimental pathology. Philippine J. Sci. Ser. B 7:173-180.

2. Loeschcke, H. 1931. Untersuchungen über die kruppöse pneumonie. Beitr. Pathol. Anat. Allg. Pathol. 86:201-230.

3. Robertson, O.H.; Coggeshall, L.T.; Terrell, E.E. 1933. Experimental pneumococcus lobar pneumonia in the dog. J. Clin. Invest. 12:467-493.

4. Williamson, J.R.; Grisham, J.W. 1961. Electron microscopy of leukocytic margination and emigration in acute inflammation in dog pancreas. Amer. J. Pathol. 39:239-256.

5. Lockwood, W.R.; Allison, F. 1963. Electronmicrographic studies of phagocytic cells. Brit. J. Exp. Pathol. 44:593-600.

6. Karrer, H.E. 1960. Electron microscopic study of the phagocytosis process in lung. J. Biophys. Biochem. Cytol. 7:357-365.

7. Majno, G.; Palade, G.E. 1961. Studies on inflammation: I. The effect of histamine and serotonin on vascular permeability; an electron microscopic study. J. Biophys. Biochem. Cytol. 11:571-605.

8. Cedergren, B. 1957. The lung tissue in mice infected by tubercle bacilli, p. 248-251. In F.S. Sjöstrand and J. Rhodin (ed.) Electron microscopy. Academic Press, New York.

9. Loosli, C.G.; Baker, R.F. 1962. Acute experimental pneumococcal (Type I) pneumonia in the mouse: The migration of leucocytes from the pulmonary capillaries into the alveolar spaces as revealed by the electron microscope. Trans. Amer. Clin. Climatol. Ass. 74:15-28.

10. Merckx, J.J.; Brown, A.L., Jr.; Karlson, A.G. 1964. An electron-microscopic study of experimental infections with acid-fast bacilli. Amer. Rev. Resp. Dis. 89:485-496.

11. Kistler, G.S.; Caldwell, P.R.B.; Wiebel, E.R. 1967. Development of fine structural damage to alveolar and capillary lining cells in oxygen-poisoned rat lungs. J. Cell Biol. 32:605-628.

12. Finegold, M.J. 1967. Interstitial pulmonary edema: An electron microscopic study of the pathology of staphylococcal enterotoxemia in rhesus monkeys. Lab. Invest. 16:912-924.

13. Petery, J.J.; Berendt, R.F.; Finegold, M.J.; Adams, H.R. October 1967. Pathogenesis of plague: I. Changes in blood coagulation during pneumonic plague in monkeys, (Technical Manuscript 415). Experimental Aerobiology Division, Fort Detrick, Frederick, Maryland.

14. Speck, R.S.; Wolochow, H. 1957. Studies on the experimental epidemiology of respiratory infections: VIII. Experimental pneumonic plague in Macaccus rhesus. J. Infect. Dis. 100:58-69.

15. Pollitzer, R. 1954. Plague. World Health Organization, Geneva. Monograph Series 22, p. 210-214.

16. Stillman, E.G. 1923. The presence of bacteria in the lungs of mice following inhalation. J. Exp. Med. 38:117-126.

17. Green, G.M.; Kass, E.H. 1964. The role of the alveolar macrophage in the clearance of bacteria from the lung. J. Exp. Med. 119:167-175.

18. Smith, P.N.; McCamish, J.; Seeley, J.; Cooke, G.M. 1957. The development of pneumonic plague in mice and the effect of paralysis of respiratory cilia upon the course of infection. J. Infect. Dis. 100:215-222.

19. Meyer, K.F. 1950. Immunity in plague: A critical consideration of some recent studies. J. Immunol. 64:139-163.

20. Domaradskii, I.V. 1966. Ocherki patogeneza chuny (Sketches of the pathogenesis of plague), Moscow. Pages 22-28.

21. Movat, H.Z.; Uriuhara, T.; Macmorine, D.L.; Burke, J.S. 1964. A permeability factor released from leukocytes after phagocytosis of immune complexes and its possible role in the Arthus reaction. Life Sci. 3:1025-1032.

22. Thomas, L. 1965. The role of lysosomes in tissue injury, p. 450-463. In B.W. Zweifach, L. Grant, and R.T. McCluskey (ed.) The inflammatory process. Academic Press, New York.

23. Orfanos, C. 1966. Mast cells and mast cell degranulation. Klin. Wochensch. 44:1277-1282.

24. Florey, H.W. 1961. The structure of normal and inflamed small blood vessels of the mouse and rat colon. Quart. J. Exp. Physiol. 46:119-122.

25. Marchesi, V.T. 1962. The passage of colloidal carbon through inflamed endothelium. Proc. Roy. Soc. London Ser. B 156:550-552.

26. Karnovsky, M.J. 1965. Vesicular transport of exogenous peroxidase across capillary endothelium into the T-system of muscle. J. Cell Biol. 27:49A.

27. Luft, J.H. 1965. The ultrastructural basis of capillary permeability, p. 121-159. In B.W. Zweifach, L. Grant, and R.T. McClusky (ed.) The inflammatory process. Academic Press, New York.

28. Sutliff, W.D.; Friedemann, T.E. 1938. A soluble edema-producing substance from the pneumococcus. J. Immunol. 34:455-467.

29. Schär, M.; Meyer, K.F. 1956. Studies on immunization against plague: XV. The pathophysiologic action of the toxin of Pasteurella pestis in experimental animals. Schweiz. Z. Allg. Pathol. 19:51-70.

30. Ajl, S.J.; Rust, J. 1960. The biochemistry and physiology of the plague murine toxin. Ann. N.Y. Acad. Sci. 88:1152-1154.

31. Snell, J.D., Jr. 1966. Effects of inhaled endotoxin. J. Lab. Clin. Med. 67:624-632.

32. Finegold, M.J.; Petery, J.J.; Berendt, R.F. October 1967. Pathogenesis of plague: II. An equivalent of the generalized Shwartzman reaction in the monkey, (Technical Manuscript 416). Pathology Division, Fort Detrick, Frederick, Maryland.

33. Finegold, Milton J. November 1967. Pathogenesis of plague: A review of plague deaths in the United States during the last decade, (Technical Manuscript 413). Pathology Division, Fort Detrick, Frederick, Maryland.

34. Walker, R.V.; Barnes, M.G.; Higgins, E.D. 1966. Composition of and physiopathology produced by plague endotoxins. Nature 209:1246.

35. Fukui, G.M.; Lawton, W.D.; Janssen, W.A.; Surgalla, M.J. 1957. Response of guinea pig lungs to in vivo and in vitro cultures of Pasteurella pestis. J. Infect. Dis. 100:103-107.

36. Burrows, T.W.; Bacon, G.A. 1954. The basis of virulence in Pasteurella pestis: Comparative behavior of virulent and avirulent strains in vivo. Brit. J. Exp. Pathol. 35:134-143.

37. Stanziale, W.G.; White, J.D. 1962. Influence of guinea pig plasma factors on phagocytosis of Pasteurella pestis: II. Plasma from plague-infected guinea pigs. J. Bacteriol. 83:182-186.

38. Janssen, W.A.; Lawton, W.D.; Fukui, G.M.; Surgalla, M.J. 1963. The pathogenesis of plague: I. A study of the correlation between virulence and relative phagocytosis resistance of some strains of Pasteurella pestis. J. Infect. Dis. 113:139-143.

39. Plummer, M.J.; Stone, R.S. 1964. The pathogenesis of viral influenzal pneumonia in mice. Amer. J. Pathol. 45:95-113.

40. Reidbord, H.E. 1957. An electron microscopic study of the alveolar-capillary wall following intratracheal administration of saline and water. Amer. J. Pathol. 50:275-289.

41. Niden, A.H.; Schulz, H. 1965. The ultrastructural effects of carbon monoxide inhalation on the rat lung. Arch. Pathol. Anat. Physiol. 339:283-292.

42. Schulz, H. 1959. The submicroscopic anatomy and pathology of the lung, p. 88-102. Springer-Verlag, Berlin.

APPENDIX

PHOTOMICROGRAPHS AND ELECTRON MICROGRAPHS

All electron micrographs appearing herein are of sections treated with a saturated solution of uranyl acetate. The meanings of the abbreviations most frequently used in the figures are:

A = alveolar lumen
C = capillary lumen
I = interstitial tissue
M = mononuclear leukocyte (monocyte, histiocyte)
P = polymorphonuclear neutrophil
bm = basement membrane

Less frequently used abbreviations are identified in the individual figure captions.

Figure 1. Pulmonary Edema. The adventitia of a vein, perivascular lymphatics, and many alveoli are distended by eosinophilic fluid. There is minimal leukocytic infiltration and focal extravasation of erythrocytes. Hematoxylin and eosin. X 68.

Figure 2. Early Lobular Pneumonia. The alveoli and alveolar ducts are filled with eosinophilic fluid containing numerous P. pestis. Neutrophils and some mononuclear leukocytes are found in modest numbers in the septa and alveoli. Hematoxylin and eosin. X 210.

Figure 3. Infected Edema Fluid. The alveolus is filled with P. pestis. There is no significant cellular exudate, and the septa appear unremarkable. Giemsa. X 1100.

Figure 4. Necrotizing Pneumonia. The alveolar architecture is obliterated. Neutrophils are abundant, and there are colonies of P. pestis in the perivascular lymphatics. Hematoxylin and eosin. X 210.

FIG. 1

FIG. 2

FIG. 3

FIG. 4

Figure 5. Intra-alveolar Bleb. A subepithelial bleb is formed by the dissection of edema fluid between the alveolar epithelial cell and the basement membrane. In this illustration, the possibility that the fluid is within an intracellular vacuole cannot be excluded. X 6400.

Figure 6. Interstitial Edema Continuity between the fluid in a similar bleb and the interstitium is shown in several places (arrows). Also there is a leukocyte within the field. X 5500.

Figure 7. Interstitial Edema and Hemorrhage. Erythrocytes are present within a bleb. Because of the plane of sectioning, continuity of the fluid with the interstitium is not seen. The figure illustrates preservation of the epithelial cell membrane, both on the side of the lumen and on that facing the basement membrane. Carbon particles are present in the capillary, but those overlying the upper erythrocyte may be an artifact. X 8000.

Figure 8. Interstitial Exudate. A capillary contains a neutrophil and monocytes. The capillary endothelial cell (En) is unremarkable. Leukocytes and erythrocytes are present in the interstitial tissue. X 4000.

FIG. 5

FIG. 6

FIG. 7

FIG. 8

Figure 9. Capillary Endothelial Damage - Early. A portion of an endothelial cell displays swelling and rarefaction of the cytoplasm. Pinocytotic vesicles are present at the basement membrane and lumenal surfaces of the cell. Mitochondria and a fragment of rough endoplasmic reticulum (arrow) appear intact. The adjacent endothelial cell (lower right) is unremarkable except for a multivesicular body (m). The junction between cells is intact. X 14,400.

Figure 10. Capillary Endothelial Damage - Early. There is focal rarefaction of the cytoplasm with formation of myelin figures. A definite encapsulating membrane around this material cannot be seen. To the right of the membranous material, a small multivesicular body is present (arrow). The basement membrane and the alveolar epithelial cell appear normal. X 21,000.

Figure 11. Capillary Endothelial Damage - Early. Osmiophilic cytoplasmic inclusions of undetermined origin are seen in a large vacuole. This clear area is apparently limited by a single membrane. The adjacent endothelial cell (right) contains a round cytoplasmic inclusion typical of lipid. Aggregates of carbon are within the lumen. No carbon was found within endothelial cells of capillaries or veins at any time. X 25,000.

Figure 12. Capillary Endothelial Damage - Late. This section was taken from an area of necrosis seen with the light microscope. There is swelling or increased electron density of endothelial cell, pericyte (per), and fibroblast cytoplasm (f). Mitochondria in the endothelial cells are swollen and vacuolated. There is fragmentation of the cell at the upper left with a gap between cells (arrow). The interstitium is edematous. X 11,800.

Figure 13. Erythrocyte Diapedesis. An erythrocyte resembles a collar button because of pinching of the cell as it passes through a gap between endothelial cells (arrow). The cytoplasm of the endothelial cells at this site appears somewhat homogeneous and is devoid of pinocytotic vesicles (compare with adjacent intact cells). X 11,800.

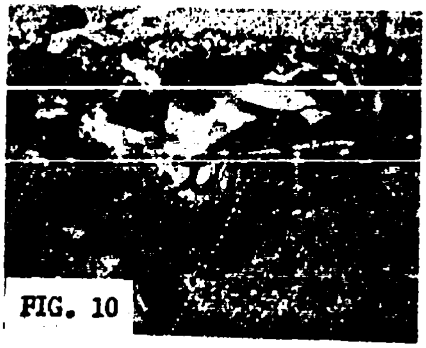

FIG. 10

FIG. 9

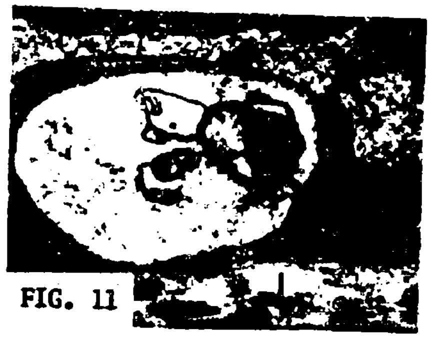

FIG. 11

FIG. 12

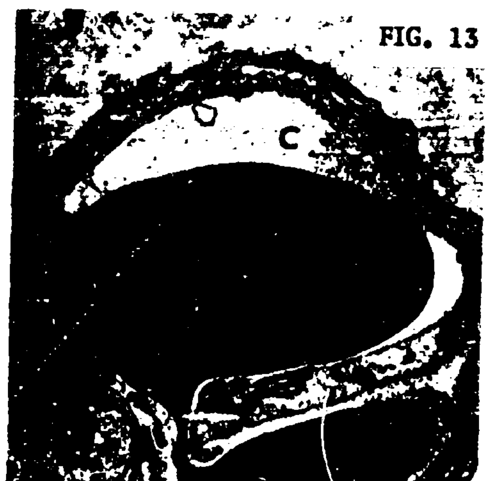

FIG. 13

Figure 14. Leukocyte Migration. A neutrophil is similarly pinched at the site of a gap in the capillary endothelium (arrows). The upper left portion of the cell is in the interstitium, while the lower right portion is still within the capillary lumen. The endothelial cells appear intact. X 9700.

Figure 15. Leukocyte Migration. A monocyte is partially outside the vessel lumen. The margins of the gap are shown by arrows. Abundant extracellular carbon accompanies the cell through the defect. X 14,400.

Figure 16. Leukocyte Migration. A neutrophil and a monocyte lie between the endothelium and the basement membrane of a capillary. The lumen of the vessel is compressed to a narrow slit (arrow) by the leukocytes. The interstitial tissue is edematous. X 5400.

Figure 17. Leukocyte Migration. The wall of a venule is shown, with the lumen (V) to the right. Neutrophils and monocytes are seen immediately beneath the intact endothelium. Another monocyte lies between the endothelial basement membrane and smooth muscle cells (arrows). X 5400.

FIG. 14

FIG. 15

FIG. 16

FIG. 17

Figure 18. Leukocyte Migration. There is a gap (arrows) in the alveolar epithelial lining, through which two neutrophils are emerging from the interstitium into the alveolar lumen. Portions of the epithelial cell cytoplasm in the area appear slightly opaque and granular. Note the absence of granules in the polymorphonuclear leukocyte at the upper left. This cell is otherwise intact and contains no phagocytized material or vacuoles in this plane of sectioning. X 7200.

Figure 19. Alveolar Exudate. The three leukocytes that comprise the cellular reaction throughout the middle and late stages of pneumonic plague are shown. At the top is a monocyte, then a neutrophil, and at the bottom an eosinophil (E) with its characteristically large, oval granules containing osmiophilic crystals. X 5400.

Figure 20. Phagocytosis. An alveolar macrophage has incorporated a neutrophil with intact granules and plague bacilli within phagocytic vacuoles. Both bacilli appear unremarkable (arrows). The granular material surrounding each bacillus may represent the capsule. Only a few lysosomes (small, round, dense cytoplasmic organelles) are present. X 9700.

Figure 21. Intracellular Digestion. Comparison of the two bacilli in this figure reveals changes in the one within the macrophage. The cytoplasm, composed chiefly of ribosomes, is relatively pale, and the nuclear material may be slightly shrunken and fragmented. The cell wall is scalloped. These changes may represent partial intracellular digestion. X 21,500.

FIG. 18

FIG. 19

FIG. 20

FIG. 21

Figure 22. Necrosis of a Phagocyte. An alveolar macrophage that had apparently contained several P. pestis shows fragmentation of the cytoplasm with disruption of the cell membrane and release of bacilli. The inner nuclear membrane has drawn away from the outer membrane, and the chromatin of the nucleus is condensed. This may represent pyknosis. A neutrophil (left) is very close to the bacilli but shows no pseudopods or phagocytic activity. X 4000.

Figure 23. Necrosis of a Phagocyte. Another example of the release of several P. pestis from a disrupted alveolar macrophage is shown. X 4000.

Figure 24. Invasion. Several P. pestis are present in the interstitium of an alveolar septum between the epithelial basement membrane and some collagen and elastic fibers (left). A granular pneumocyte (right) shows multiple vacuoles and dilated endoplasmic reticulum (arrows) in addition to the usual osmiophilic inclusions. X 14,400.

Figure 25. Epithelial Degeneration. The alveolar epithelial cell at the upper left contains swollen mitochondria and several round, membrane-bound inclusions within a rarefied cytoplasmic matrix. Rarefaction is also found in the epithelial cell to the right. The interstitium is markedly edematous. X 9000.

Figure 26. Epithelial Sloughing. Denuded basement membrane is shown at the upper left (arrow). A remnant of a granular, opacified epithelial cell covers the membrane to the right. The capillary endothelium is intact. X 14,400.

Figure 27. Mast Cell. A normal mast cell is found in the edematous adventitia of a vein early in the disease. X 5400.

Figure 28. Mast Cell Degranulation. The granules of the mast cell retain their structural integrity but appear empty. The interstitium is edematous. This was from an area of more advanced inflammation. X 5400.


FIG. 22


FIG. 24

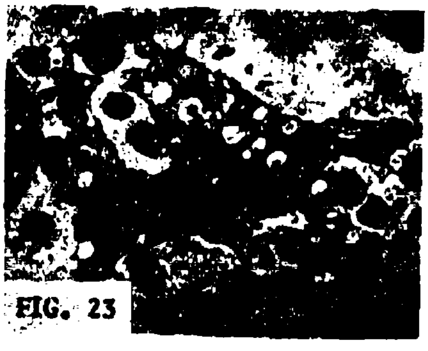
FIG. 23

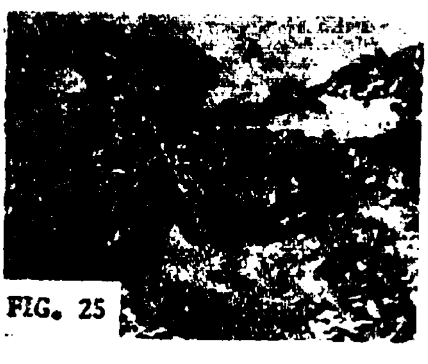
FIG. 25

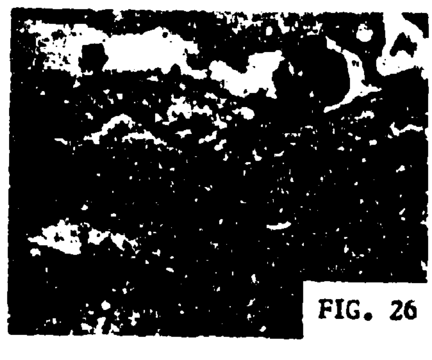
FIG. 26

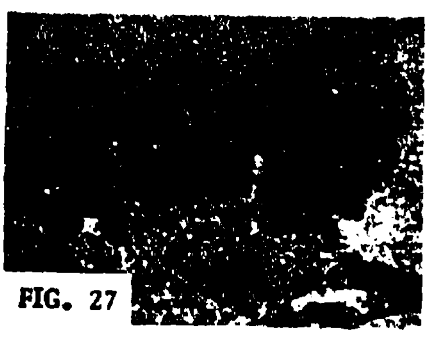
FIG. 27

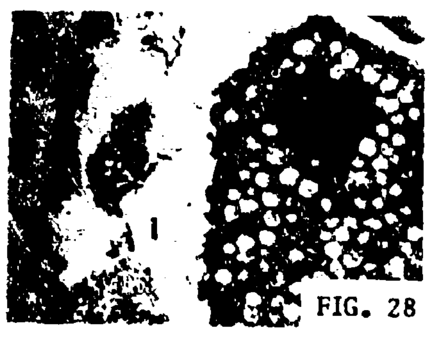
FIG. 28

DOCUMENT CONTROL DATA - R & D

(Security classification of title, body of abstract and indexing annotation must be entered when the overall report is classified)

1. ORIGINATING ACTIVITY (Corporate author)
Department of the Army
Fort Detrick, Frederick, Maryland, 21701

2a. REPORT SECURITY CLASSIFICATION
Unclassified

2b. GROUP

3. REPORT TITLE
PNEUMONIC PLAGUE IN MONKEYS: AN ELECTRON MICROSCOPE STUDY

4. DESCRIPTIVE NOTES (Type of report and inclusive dates)

5. AUTHOR(S) (First name, middle initial, last name)
Milton J. Finegold

6. REPORT DATE	7a. TOTAL NO. OF PAGES	7b. NO. OF REFS
February 1968	35	42

8a. CONTRACT OR GRANT NO.

b. PROJECT NO. 1C5223C1A059

c.

d.

9a. ORIGINATOR'S REPORT NUMBER(S)
Technical Manuscript 430

9b. OTHER REPORT NO(S) (Any other numbers that may be assigned this report)

10. DISTRIBUTION STATEMENT
Qualified requesters may obtain copies of this publication from DDC.
Foreign announcement and dissemination of this publication by DDC is not authorized.
Release or announcement to the public is not authorized.

11. SUPPLEMENTARY NOTES

12. SPONSORING MILITARY ACTIVITY
Department of the Army
Fort Detrick, Frederick, Maryland, 21701

13. ABSTRACT

The infection of monkey lungs by *Pasteurella pestis* was studied with the electron microscope. The disease was first apparent clinically at 60 to 70 hours and pathologically at 72 hours. At this time, the initial response seen with the light microscope was alveolar edema with massive proliferation of organisms. With the electron microscope, interstitial edema around veins and bronchi was the earliest observed response to the presence of numerous intra-alveolar bacilli. Early in the disease, before the onset of a leukocytic exudate, interstitial fluid also accumulated in the form of subepithelial blebs. No evidence of significant vascular damage was found to account for the marked increase in permeability, even with the aid of intravenous injections of colloidal carbon prior to sacrifice. Leukocytic and mast cell factors in the pathogenesis of the edema appear unlikely. Once the cellular component of the reaction developed, *P. pestis* resisted both phagocytosis by polymorphonuclear neutrophils and intracellular digestion by mononuclear phagocytes. Invasion of the tissues by the organism was observed only in the advanced stages of the pneumonia, when all components of the alveolar septa were undergoing necrosis.

14. Key Words

*Monkeys
*Plague
*Electron microscopes
Pasteurella pestis
Edema

DD FORM 1 NOV 65 1473 REPLACES DD FORM 1473, 1 JAN 64, WHICH IS OBSOLETE FOR ARMY USE.